Eurographics Workshop on Visual Computing for Biomedicine (2008)
C. P. Botha, G. Kindlmann, W. J. Niessen, and B. Preim (Editors)

Computation and Visualization of Asynchronous Behavior of the Heart

S. Wesarg[1], C. Lacalli[2]

[1]Technische Universität Darmstadt, Dept. of Computer Science, GRIS, Germany
[2]Fraunhofer IGD, Dept. Cognitive Computing & Medical Imaging, Germany

Abstract

Nowadays, computer-aided diagnosis is widely used in the analysis of cardiac image data. Especially, for the investigation of the dynamic behavior of the heart, automated analysis tools for 4D data sets have been developed. A small set of descriptors of the heart's dynamics are established and used in the clinical routine. However, there exists a whole lot more of such parameters that can be extracted by analyzing 4D data sets. But, many of them are not used due to several reasons: time-consuming computation, no intuitive meaning, little clinical relevance, etc.. In this work we propose a novel descriptor for the dynamic behavior of the heart that can easily be computed from 4D data sets. It describes to which extent the heart exhibits an asynchronous movement. This novel descriptor ASYNCHRONISM *is based on the already established measures* WALL MOTION *and* WALL THICKENING*, but reveals new, valuable information that is not available when relying only upon the two aforementioned parameters. The* ASYNCHRONISM *has an intuitive meaning, since it corresponds to the clinical classification scheme of wall motion abnormalities. Beyond its computation we present in this work also methods for its visualization as well as first preliminary results for 4D cardiac magnetic resonance image data.*

Categories and Subject Descriptors (according to ACM CCS): J.3 [Life and Medical Sciences]: Health

1. Introduction

Cine magnetic resonance imaging (MRI) is the standard for the examination of cardiac dynamics [CLB03, PRW*04]. MRI systems provide 4D data (volume + time) enabling the cardiologist to study the movement of the myocardial muscle. There, especially the left ventricle (LV) is of high interest due to its importance for the systemic circulation of the blood. A diseased LV represents a severe danger for the patient's health. Thus, an early detection of any abnormalities of left ventricular motion is important for saving life.

During the past three decades, many parameters for modeling the cardiac shape and its deformation and movement have been proposed [FNV01]. In order to generate those models, the cardiac boundaries have to be extracted from the image data. The simplest approach is a manual delineation of inner and outer borders of the myocardium directly in the image data. Considering the fact that a 4D cine data set consists of 20 up to 35 volumes, each containing 8 to 12 slices (in case of short-axis MRI data), it is obvious that this time-consuming and error-prone task requires automation.

Several methods have been successfully applied to the extraction of left ventricular boundaries: the already mentioned manual drawing of an initial contour and its automatic adaptation [HLBG06]; employing level set methods [CLC*05, LGW08] and active contours [PMWH05]; the generation and utilization of shape models [vADF*06] and AAMs [AOH*07]. However, the discussion of these approaches is beyond the scope of this paper, and the reader is referred to the literature.

Once, the cardiac contours are extracted, the change and movement of these boundaries over time can be studied. First, there exist global volumetric parameters: *stroke volume*, *cardiac output*, and *ejection fraction* (EF). Second, there are measures for describing the movement and the deformation of the cardiac wall: *wall motion* (WM) and *wall thickening* (WT) [HBdR*97, FNV01]. Finally, there exist some 'exotic' parameters [PFZ*05, ZTW*07]. WM and WT as established parameters can be used for the classification of (regional) abnormal movement of the left ventricle. For the description of the diseased myocardium one distin-

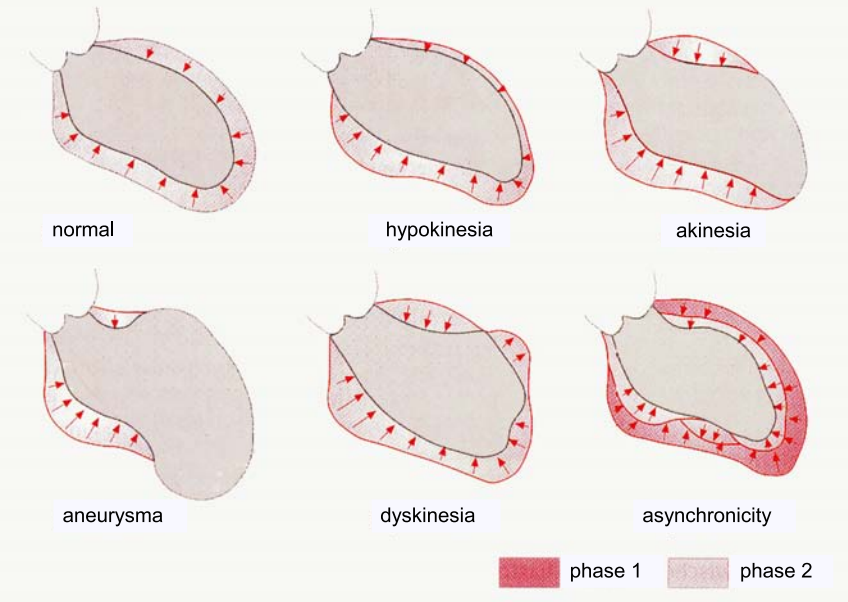

Figure 1: *The classification of wall motion abnormalities based on their characteristic motion patterns. (Image taken from [Kös04] and modified by the authors.)*

guishes between a restricted mobility (hypokinesia), a halt during systole and diastole (akinesia), a systolic movement outwards (dyskinesia), motion out of sync (asynchronicity), and a ventricular aneurysma (a dilation of the ventricle's wall) [Kös04] (fig. 1).

In this work we present a novel descriptor for the LV dynamics called *asynchronism*. It is based on the aforementioned parameters WM and WT. In the past, the quantification of asynchronous behavior of the heart has already been investigated [BS90]. However, this early approach was based on 2D X-ray cine-ventriculograms. To the knowledge of the authors there has not been published any work renewing Bolson's ideas and dealing with the automated extraction and visualization of information regarding asynchronous behavior based on state-of-the-art MRI data.

In the following, we will explain what the parameter asynchronism represents and how it can be computed from cine MRI data. We will present means for its visualization, and show first examples related to the detection of wall motion abnormalities.

2. Methods

The computation of asynchronous behavior of the heart, in particular the LV, requires knowledge about the location of inner (endocardium) and outer wall (epicardium) for all volumes of the cine MRI data set. Thus, these two boundaries have to be extracted first. Furthermore, we want to detect pathological regions of the ventricle. Consequently, the LV has to be divided into several meaningful segments [CWD*02]. The computation of asynchronism, as we propose in this work, is based on the time curves related to WM and WT and the change in left ventricular volume over time. Once these time curves are computed, the asynchronism for each of the LV regions can be calculated. Finally, the results must be presented to the cardiologist in a convenient manner. Here, we adhere to recommendations for a standardized presentation of analysis results for the LV [CWD*02].

2.1. Prerequisites

Describing asynchronous behavior of the heart is quantification of its dynamics. Thus, all computations are based on cine MRI data, containing a certain number of volumes that cover the whole cardiac cycle. For our work, we deal with clinically relevant cine MRI data that is organized as stacks of short-axis slices for each point in time. These 8 to 12 slices being oriented perpendicular to the long axis cover the LV completely from the plane of the mitral valves (MV) to the heart's apex (fig. 2). During one cardiac cycle, 20 to 35 such volume stacks are acquired representing a sufficient temporal resolution for analyzing the dynamics.

We base the measurement of asynchronism on WM and WT calculation. In order to compute the latter ones, the location of endocardial and epicardial border has to be known. This information is obtained by means of segmentation. No matter which approach has been chosen (see section 1) the segmentation result consists of two contours – one for the

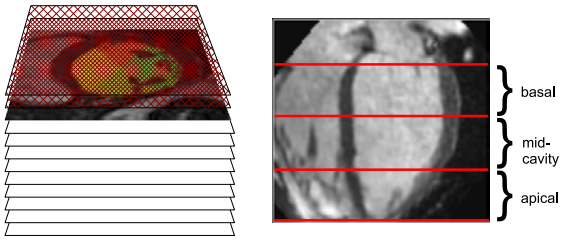

Figure 2: *Volume data organized as a stack of short-axis slices, that are all oriented perpendicular to the left ventricular long axis (*left*). In order to analyze such data, this stack is split up into three equally sized regions along the long axis (*right*, see also [CWD*02]).*

endocardial and a second one for the epicardial border. WM is usually computed as the movement of the endocardial wall towards and away from a reference position – usually the location of the left ventricular long axis [FNV01].

For a subsequent analysis, the LV can be divided into 17 segments following the nomenclature of the *American Heart Association* (AHA) [CWD*02]. Therefore, the stack of short-axis slices is split up into three equally sized regions – basal, mid-cavity and apical (fig. 2). Each of these regions is further divided into 6 (basal and mid-cavity) resp. 4 (apical) segments, and the region below the apical region – the apex – is added.

For each segment k, $k = 1,\ldots,16$ (apex not considered) the same number of $M \times N$ equally spaced endocardial positions can be computed – representing the spatial resolution for the parameter computation. The radial distances $d_k^i(m,n)$ from the long axis position for these locations can be calculated for all points in time i. Averaging over all distances that belong to one segment, at a specific point in time, the mean distance is then given by

$$\overline{d}_k^i = \frac{\sum_{n=0}^{N-1}\sum_{m=0}^{M-1} d_k^i(m,n)}{M \cdot N}. \qquad (1)$$

This results in time curves representing the temporal change of distance over the cardiac cycle for each segment (fig. 3).

WT is based on the measurement of myocardial thickness. The latter one can be calculated as the distance between two corresponding endocardial and epicardial positions. The classical approach for this is the centerline method [SBD*86] and its improvements [vRvdWS*94, vdGdRvdWR97, HBdR*97]. Small line segments called *chords* are drawn perpendicular to the line that is equidistant to the endocardial and the epicardial boundaries of the same short-axis slice – the centerline. Assuming that we have $M \times N$ such chords computed, their corresponding lengths determine the myocardial thickness $MT_k^i(m,n)$ at position (m,n) of segment k at phase i of the cardiac cycle. The average value for each segment, at a specific point in time, is

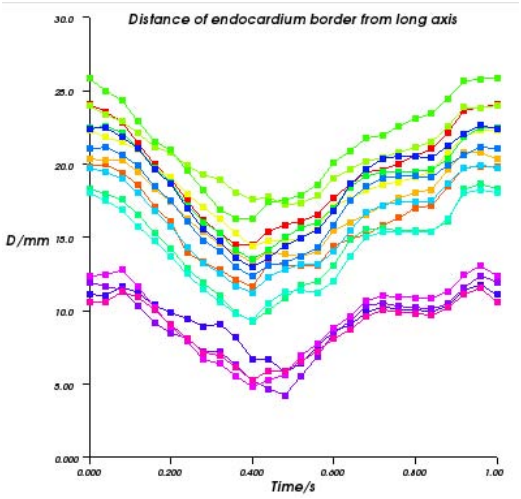

Figure 3: *Time curves for the change of the endocardial distances for all* 16 *segments of basal, mid-cavity and apical region.*

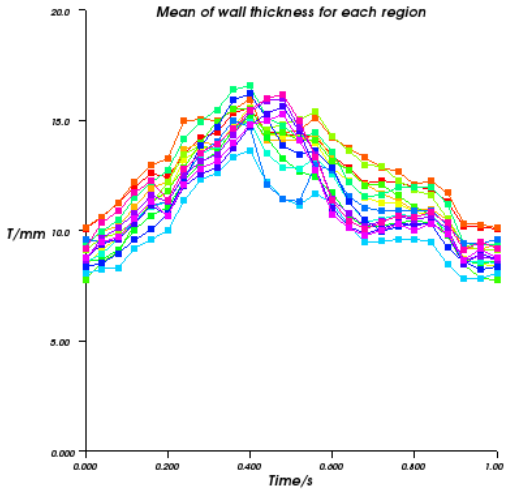

Figure 4: *Time curves for the change of the myocardial thickness for all* 16 *segments of basal, mid-cavity and apical region.*

then given by

$$\overline{MT}_k^i = \frac{\sum_{n=0}^{N-1}\sum_{m=0}^{M-1} MT_k^i(m,n)}{M \cdot N}. \qquad (2)$$

Similar to the distance computation, time curves for the myocardial thickness can be generated (fig. 4).

Finally, two characteristic points in time regarding the cardiac cycle have to be computed. These are the end-diastole (ED) and the end-systole (ES). ED represents the moment where the LV is maximally filled with blood, whereas ES

indicates the moment of maximum contraction before the filling of the LV starts again. Thus, if the LV volume is measured, ED and ES can be extracted from the cine data as the moment with a maximum resp. a minimum left ventricular volume. Based on the edocardial border location this can easily be done by simply counting all voxels that are inside this boundary and a multiplication with the voxel size.

Once we have done this final computation, we have gathered all information necessary for computing the asynchronism. (For the sake of completeness: The increase of the endocardial distance between ES and ED defines the corresponding value for WM. And the increase of the myocardial thickness from ED to ES in relation to the end-diastolic myocardial thickness gives the WT value.)

2.2. Computation of asynchronism

WM and WT as established descriptors allow for a detection of wall motion abnormalities that are related to an insufficient motion of the left ventricular wall. However, deviations in the motion patterns are not easily detectable. In order to provide a means for this, we propose the following scheme for quantifying asynchronous behavior of the LV.

The two moments ED and ES of the cardiac cycle characterize the transition from one motion state to an other, and we build our argumentation on them. Recalling the wall motion abnormalities (section 1), we can now think about how the time curves for distance and myocardial thickness are expected to look like. If segments of the LV are not in sync with the main part of the myocardial muscle, the minimum resp. maximum of these time curves will not correspond to the ED resp. ES. But, a normal wall motion is characterized by the following: the maximum distance of the endocardial border from the long axis occurs at ED, the maximum myocardial thickness coincides with the ES, and vice versa for the corresponding minima.

Consequently, a manifestation of wall motion abnormalities would be the case where minima resp. maxima of the already mentioned time curves do not correspond to ED and ES. *Asynchronism of wall motion* we define as the deviation of the moment $t\left[d_k(m,n)\right]_{max}$, where the maximum endocardial distance

$$d_k(m,n)|_{max} = \max\left[d_k^i(m,n)\right]\Big|_{\forall i} \tag{3}$$

is reached, from $t^{ED}\left[d_k(m,n)\right]$, the end-diastole:

$$A_k(m,n)|_{WM} := \frac{t^{ED}\left[d_k(m,n)\right] - t\left[d_k(m,n)\right]_{max}}{t^{cycle}} \times 100\,\% \tag{4}$$

The length of the cardiac cycle is denoted with t^{cycle}. (An alternative definition could be based on considering the minimum distance and its deviation from ES.)

In a similar manner we define the *asynchronism of wall thickening* as the deviation of the moment $t\left[MT_k(m,n)\right]_{max}$ with maximal myocardial thickness

$$MT_k(m,n)|_{max} = \max\left[MT_k^i(m,n)\right]\Big|_{\forall i} \tag{5}$$

from $t^{ES}\left[MT_k(m,n)\right]$, the end-systole:

$$A_k(m,n)|_{WT} := \frac{t^{ES}\left[MT_k(m,n)\right] - t\left[MT_k(m,n)\right]_{max}}{t^{cycle}} \times 100\,\% \tag{6}$$

(Again, an alternative definition could be based on considering the minimum myocardial thickness and its deviation from ED.) Fig. 5 illustrates the above definitions.

2.3. Visualization of asynchronous behavior

Regions that show an asynchronous behavior should be easily recognizable, and the quantitative extent of asynchronism should be accessible as well. We decided to use a standard way for visualizing the results of the asynchronism computation. There, we adhere to the AHA recommendations [CWD*02] and use a bull's-eye display (figs. 6 and 7). The mapping of the values to the used color gradient (hue 0.0 to 0.66 in HSV color space) is as follows:

- -30% and below: red,
- 0%: green,
- 30% and above: blue.

Thus, normal-kinetic regions are greenish, whereas regions showing an asynchronous behavior are more reddish resp. bluish.

3. Results

The above presented approach is not yet clinically evaluated. We only did preliminary tests with a limited number of clinical cine MRI data sets, and two examples are shown below. The image data originated from different hospitals and was acquired employing MRT scanners from different manufactures (*Philips* and *Siemens*). It consisted of 20 to 25 single volumes covering the whole cardiac cycle. The in-plane resolution was approx. $1.5 \times 1.5\,mm^2$, and the slice thickness ranged from 5 to $8\,mm$.

In order to verify the outcome of our method, we used the clinical diagnosis results for these image data sets. The examination of that data had been done by experienced cardiologists in a purely visual manner by inspecting all short-axis slices in 2D cine mode. The output of our analysis was composed of bull's-eye displays for the two types of asynchronism calculations and the classical descriptors WM and WT as well as the aforementioned time curves for endocardial distance, myocardial thickness, and global volumetry.

For the limited number of data sets it could be observed that regions with distinctive features in the bull's-eye displays for WM and WT, showed a noticeable coloring also for the two types of asynchronism. Furthermore, there where

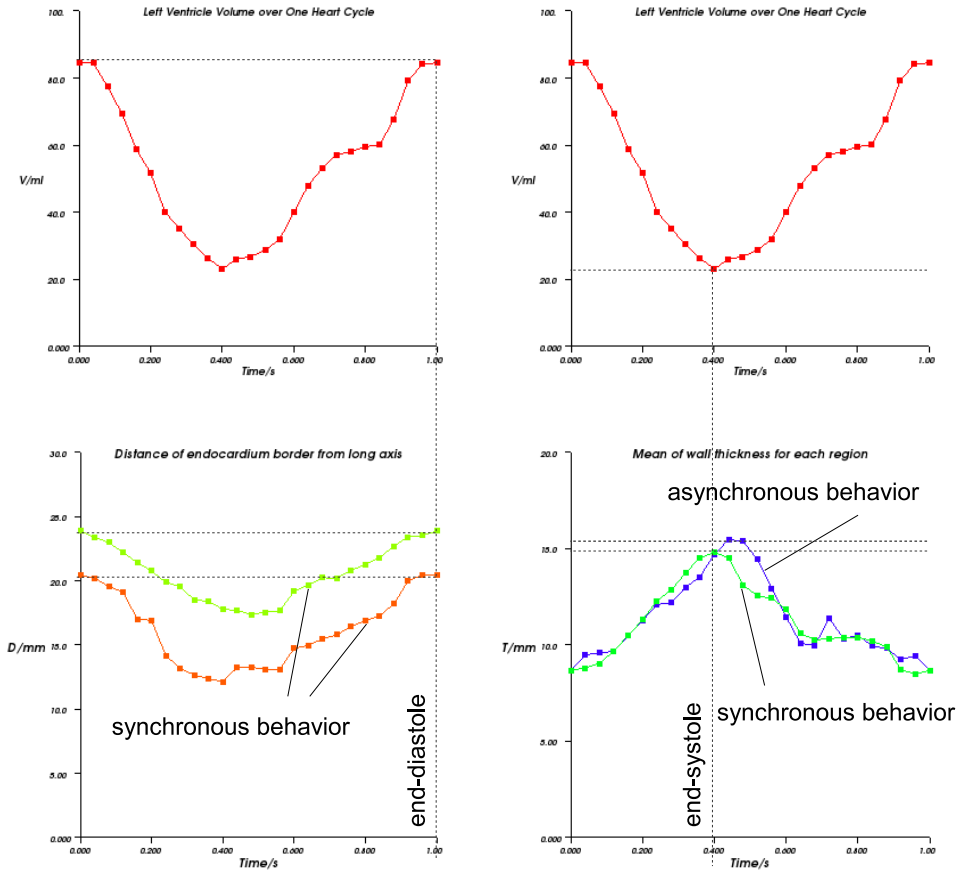

Figure 5: *The computation of asynchronism is based on ED and ES that are derived from global volumetric calculations. The novel descriptor can be defined taking wall motion resp. wall thickening into account. In the first place the deviation of the moment with a maximum endocardial distance from the ED is considered, for the latter case it is the deviation of the moment with maximal myocardial thickness from ES.*

regions labeled by the cardiologists to be pathological, i.e., showing wall motion abnormalities, but, the display of WM and WT did not always correspond to these diagnosis results. Unlike these classical descriptors, the newly introduced asynchronism showed a much better accordance to the clinical diagnosis.

Figures 6 and 7 show two examples for the analysis results of two different data sets. The first one is for a patient who is considered to be without any cardiac malfunction. We provide this figure in order to show that in case of a healthy patient – at least for the shown case – the newly introduced parameter leads to an analysis result that, in correspondence with the parameter WM, correctly reflects the absence of wall motion abnormalities. However, in the second example, a cardiologist diagnosed the patient with several regions of abnormal wall motion. Here, unlike to WM and WT, the asynchronism correctly labeled these regions as performing an asynchronous motion.

4. Discussion

We have presented a method for an automatic computation of asynchronous behavior of the heart. This newly introduced descriptor for left ventricular dynamics should be advantageous compared to the classical descriptors WM and WT in the case of wall motion abnormalities. The main focus of this work was on the development of the methodology; not yet a full-blown quantitative comparison with a huge number of data sets. Preliminary tests with only a few data sets indicated that regions that are not classified by WM and WT to be pathological show distinctive features when asynchronism is considered. These are very encouraging results, however, a real clinical study with a larger number of patients has to be done. An ongoing collaboration with the *Johann Wolfgang Goethe University Hospital* in Frankfurt/M., Germany, gives this opportunity, and a clinical evaluation of the newly introduced method is already planned.

The introduction of the novel descriptor asynchronism is

an attempt to establish an objective method for detecting and quantifying wall motion abnormalities. The increasing amount of data that is acquired during a routine examination of the heart makes it necessary to overcome the (up to now only) visual detection of asynchronous behavior of the heart, and there especially the LV. Bolson et al. [BS90] pioneered the quantification of asynchronous behavior of the LV borders. But, their work was based on 2D X-ray cine ventriculograms. With this work, we renewed their ideas and adapted them to the state-of-the-art in dynamic cardiac imaging – cine MRI. Adhering to this imaging modality as well as to the standardized nomenclature introduced by the AHA [CWD*02] makes our approach immediately understandable for cardiologists and therefore useable in the clinical environment. Furthermore, it ensures its comparability to other (existing) approaches. In addition, the meaning of asynchronism is easy to grasp, and therefore the acceptance among clinicians should be higher than it is for more technically driven parameters like for instance PCA modes [ZTW*07].

We also want to discuss some limitations of our approach. First of all, the analysis result is heavily depending on good segmentation results. If the endocardial borders are not correctly delineated, the computed values for LV volume may be incorrect. This could then lead to a false determination of ED and ES, since the time frames surrounding these phases differ only marginally. It is obvious, that this would have a large effect on the computation of asynchronism. Another item is the question, which abnormal motion patterns (fig. 1) can be detected if our method is employed. It is evident, that dyskinesia and asynchronicity represent motion patterns that can perfectly be traced. However, the question if hypokinesia and akinesia always exhibit a characteristic influence on the computed value for asynchronism – as may be derived from one of the given examples – remains an open question. And this has to be answered during a clinical study.

Furthermore, several improvements could be done. The computation of asynchronism as proposed in this work makes it not possible to distinguish between different wall motion abnormalities (sec. 1). Here, additional work has to be done. Another extension concerns the way of visualizing the results. Currently, we use bull's-eye displays following the AHA recommendations [CWD*02]. A more intuitive approach would be the color-coded mapping of the computed values to a 3D visualization of the left ventricle as proposed by several groups [EMRR01, WN06].

5. Conclusions

Cardiac imaging highly demands diagnosis tools for an automated analysis of the increasing amount of image data. The extraction of important cardiac structures is one field where a lot of progress has been made over the past years. However, it is also important for the clinical routine to get the most out of these segmentation results. Currently, all analysis of dynamic image data is based on only a few parameters (WM, WT, and EF). The introduction of asynchronism is a natural extension that is partially based on the computation of these parameters. We are convinced that this novel descriptor will show its clinical usefulness due to its diagnostic value and its intuitive meaning.

6. Acknowledgment

We want to thank the University Hospitals in Frankfurt/M. and Heidelberg as well as the Hospital Offenbach for providing us image data and diagnosis results. This work has been supported by the *German Heart Foundation*, research grant *F/26/05 rev*.

References

[AOH*07] ANGELIÉ E., OOST E. R., HENDRIKSEN D., DER GEEST B. P. L. R. J. V., REIBER J. H.: Automated contour detection in cardiac MRI using active appearance models: the effect of the composition of the training set. *Invest Radiol. 42*, 10 (2007), 697–703.

[BS90] BOLSON E. L., SHEEHAN F. H.: Quantification of asynchronous displacement of heart borders. In *Computers in Cardiology, Proceedings* (1990), pp. 613–616.

[CLB03] CASTILLO, MD E., LIMA, MD J. A. C., BLUEMKE, MD, PHD D. A.: Regional Myocardial Function: Advances in MR Imaging and Analysis. *Radiographics 23*, Special Issue (2003), 127–140.

[CLC*05] CORSI C., LAMBERTI C., CATALANO O., MACENEANEY P., BARDO D., LANG R. M., CAIANI E. G., MOR-AVI V.: Improved Quantification of Left Ventricular Volumes and Mass Based on Endocardial and Epicardial Surface Detection From Cardiac MR Images Using Level Set Models. *J Cardiovasc Magn Reson 7*, 3 (2005), 595–602.

[CWD*02] CERQUEIRA M. D., WEISSMAN N. J., DILSIZIAN V., JACOBS A. K., KAUL S., LASKEY W. K., PENNELL D. J., RUMBERGER J. A., RYAN T., VERANI M. S.: *Standardized Myocardial Segmentation and Nomenclature for Tomographic Imaging of the Heart*. Circulation 105:539–542, American Heart Association, Inc., 2002. http://www.circulationaha.org.

[EMRR01] EUSEMANN C. D., MOHLENKAMP S., RITMAN E. L., ROBB R. A.: 3D Quantitative Visualization of Altered LV Wall Thickening Dynamics Caused by Coronary Microembolization. In *Medical Imaging 2001* (2001), vol. 4321 of *Proc. of SPIE*, pp. 100–107.

[FNV01] FRANGI A. F., NIESSEN W. J., VIERGEVER M. A.: Three-Dimensional Modeling for Functional Analysis of Cardiac Images: A Review. *IEEE Trans Med Imaging 20*, 1 (January 2001), 2–25.

[HBdR*97] HOLMAN E. R., BULLER V. G. M.,

DE ROOS A., VAN DER GEEST R. J., BAUR L. H. B., VAN DER LAARSE A., BRUSCHKE A. V. G., REIBER J. H. C., VAN DER WALL E. E.: *Detection and quantification of dysfunctional myocardium by magnetic resonance imaging: A new three-dimensional method for quantitative wall-thickening analysis*. Circulation 95:924–931, American Heart Association, Inc., 1997. http://www.circulationaha.org.

[HLBG06] HAUTVAST G., LOBREGT S., BREEUWER M., GERRITSEN F.: Automatic contour propagation in cine cardiac magnetic resonance images. *IEEE Trans Med Imaging 25*, 11 (2006), 1472–1482.

[Kös04] KÖSTER R.: A Small Primer on the Clinical Use of MSCT for Heart Exams. *TOSHIBA Visions*, 5 (2004), 6–11.

[LGW08] LYNCH M., GHITA O., WHELAN P. F.: Segmentation of the left ventricle of the heart in 3-D+t MRI data using an optimized nonrigid temporal model. *IEEE Trans Med Imaging 27*, 2 (2008), 195–203.

[PFZ*05] PILGRAM R., FRITSCHER K. D., ZWICK R.-H., SCHOCKE M. F., TRIEB T., PACHINGER O., SCHUBERT R.: Shape analysis of healthy and diseased cardiac ventricles using PCA. In *Computer Assisted Radiology and Surgery* (2005), Lemke H. U., (Ed.), Proc. of the 19th CARS 2005, Elsevier, pp. 357–362.

[PMWH05] PLUEMPITIWIRIYAWEJ C., MOURA J. M., WU Y. J., HO C.: STACS: new active contour scheme for cardiac MR image segmentation. *IEEE Trans Med Imaging 24*, 5 (2005), 593–603.

[PRW*04] PUJADAS S., REDDY G. P., WEBER O., LEE J. J., HIGGINS C. B.: MR Imaging Assessment of Cardiac Function. *J Magn Reson Imaging 19*, 6 (June 2004), 789–799.

[SBD*86] SHEEHAN F. H., BOLSON E. L., DODGE H. T., MATHEY D. G., SCHOFER J., WOO H. W.: Advantages and applications of the centerline method for characterizing regional ventricular function. *Circulation 74*, 2 (1986), 293–305. http://www.circulationaha.org.

[vADF*06] VAN ASSEN H. C., DANILOUCHKINE M. G., FRANGI A. F., ORDÁS S., WESTENBERG J. J., REIBER J. H., LELIEVELDT B. P.: SPASM: a 3D-ASM for segmentation of sparse and arbitrarily oriented cardiac MRI data. *Med Image Anal. 10*, 2 (2006), 286–303.

[vdGdRvdWR97] VAN DER GEEST R. J., DE ROOS A., VAN DER WALL E. E., REIBER J. H. C.: Quantitative analysis of cardiovascular MR images. *Int J Card Imag 13* (June 1997), 247–258.

[vRvdWS*94] VAN RUGGE F. P., VAN DER WALL E. E., SPANJERSBERG S. J., DE ROOS A., MATHEIJSSEN N. A., ZWINDERMAN A. H., VAN DIJKMAN P. R., REIBER J. H., BRUSCHKE A. V.: Magnetic resonance imaging during dobutamine stress for detection and localization of coronary artery disease. Quantitative wall motion analysis using a modification of the centerline method. *Circulation AHA 90*, 1 (1994), 127–138.

[WN06] WESARG S., NOWAK S.: An Automated 4D Approach for Left Ventricular Assessment in Clinical Cine MR Images. In *Informatik 2006. Informatik für Menschen. Band 1* (2006), Hochberger C., Liskowsky R., (Eds.), vol. P-93 of *GI-Lecture Notes in Informatics*, pp. 483–490.

[ZTW*07] ZHANG H., THOMAS M. T., WALKER N. E., STOLPEN A. H., WAHLE A., SCHOLZ T. D., SONKA M.: Four-dimensional functional analysis of left and right ventricles using MR images and active appearance models. In *Medical Imaging 2007* (2007), Manduca A., Hu X. P., (Eds.), vol. 6511 of *Proc. of SPIE*.

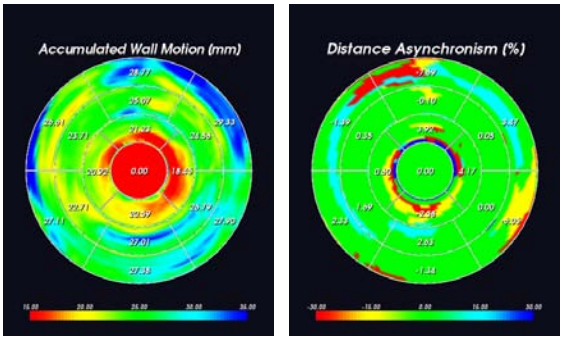

Figure 6: *Evaluation results for a patient who is considered to be without any cardiac malfunction. Only the bull's-eye displays for WM and the thereon based asynchronism are shown. One can easily perceive the relative homogeneous greenish coloring in both cases.*

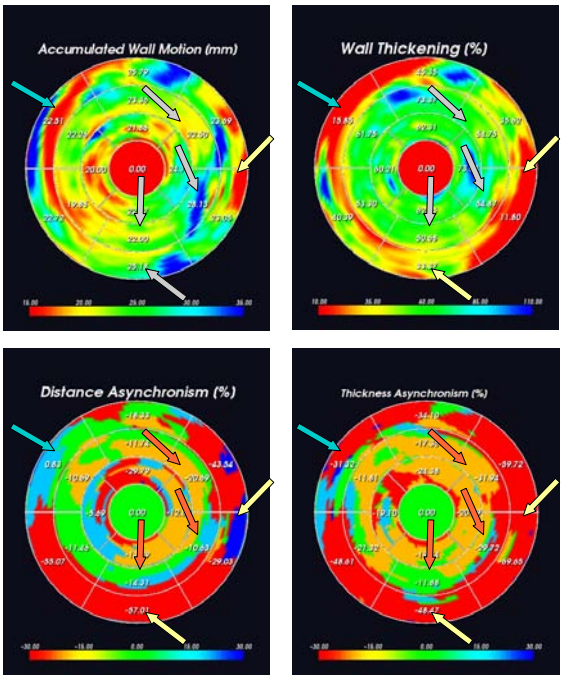

Figure 7: *Evaluation results for a patient with wall motion abnormalities detected in 2D cine images. The cardiologist's diagnosis was as follows:* mid-cavity *– hypokinesia anterolateral and inferior, akinesia inferolateral (orange arrows);* basal *– hypokinesia inferior, akinesia lateral (yellow arrows). It can be seen that the established descriptors WM and WT do not well reproduce this reference diagnosis. The regions indicated by a gray arrow do not show distinctive features. However, the novel descriptor asynchronism correctly highlights these pathological regions. Open question remains the fact that all descriptors reveal an abnormality in the basal anteroseptal segment (blue arrow), that has not been labeled as being pathological by the cardiologist.*